Available online at www.sciencedirect.com

ScienceDirect

MATTER AND RADIATION AT EXTREMES

Matter and Radiation at Extremes 1 (2016) 123−131

www.journals.elsevier.com/matter-and-radiation-at-extremes

Research article

Validation for equation of state in wide regime: Copper as prototype

Haifeng Liu*, Haifeng Song, Qili Zhang, Gongmu Zhang, Yanhong Zhao

Laboratory of Computational Physics, Institute of Applied Physics and Computational Mathematics, Beijing 100088, China

Received 14 September 2015; revised 4 January 2016; accepted 27 January 2016
Available online 29 March 2016

Abstract

In this paper we introduce the wide regime equation of state (WEOS) developed in Institute of Applied Physics and Computational Mathematics (IAPCM). A semi-empirical model of the WEOS is given by a thermodynamically complete potential of the Helmholtz free energy which combines several theoretical models and has some adjustable parameters calibrated via some experimental and theoretical data. The validation methods of the equation of state in wide regime are presented using copper as a prototype. The results of the WEOS are well consistent with the available theoretical and experimental data, including ab initio cold curve under compression, isotherm, Hugoniot, off-Hugoniot and sound velocity data. It enhances our confidence in the accuracy of the WEOS, which is very important for the validation and verification of equation of state in high temperature and pressure technology.

PACS codes: 05.70.Ce; 64.30.Ef; 64.30.-t

Keywords: Validation; Wide-range equation of state; Copper; Ab initio cold curve; Room-temperature isotherm; Hugoniot; Velocity of sound

1. Introduction

The states and thermodynamic properties of matter are described by equation of state (EOS). EOS is of immediate interest in astrophysics, planetary physics, power engineering, controlled thermonuclear fusion, impulse technologies, engineering, and several special applications [1]. Numerous techniques and models have been developed for obtaining EOS of a variety of materials which are valid up to very extreme pressure (tens of Mbar) and temperature (several eV or even higher). The predominant methods to obtain EOS experimental data are through dynamic shock wave compression [2], static compression [3] and techniques that couple static and dynamic compression [4]. There are many models based on first-principle theories, such as Thomas-Fermi model [5] with various corrections [6,7], Hartree-Fock-Slater model [8], plasma [9] and liquid state models [10], models derived from Quantum Molecular Dynamic [11−14] and Quantum Monte Carlo [15−17] method. But until now none of them is universal in the wide regime and only applicable in a relatively limited regime. For this reason, the semi-empirical EOS models [1,18,19], where the functional form is motivated by sound theoretical results and the adjustable parameters are tuned to numerous experimental data at high pressure and temperature, have played a very significant role in numerous applications. Within the high-energy-density-physics community, multi-phase wide-range EOS [1], SESAME [18], and QEOS [19], which have been derived by scientists with the use of different physical assumptions and experiments, are widely referenced. In fact, the WEOS, which is accurate in wide regime, has been widely used in IAPCM for many years.

In this paper, we introduce the WEOS developed in IAPCM and take copper as an example to illustrate the performance of the WEOS.

* Corresponding author.
E-mail address: liu_haifeng@iapcm.ac.cn (H. Liu).
Peer review under responsibility of Science and Technology Information Center, China Academy of Engineering Physics.

http://dx.doi.org/10.1016/j.mre.2016.03.002

The theoretical model of WEOS is briefly described in Sec. 2. In Sec. 3 the validation of the EOS under extreme conditions of pressure and temperature is given, and the results for copper are presented. Finally, we summarize the state of the art of WEOS.

2. Theoretical model

Since some fundamental difficulties have not been overcome, a universal and rigorous theoretical model for describing the wide range thermodynamic properties of matter still does not exist. As we know, only very basic and limited results can be obtained using models based on simplified assumptions on the structure, energy spectrum, and the nature of the interaction between particles. Via the combination and modification of several existing models, similar to the case for the SESAME, we proposed a method to obtain the WEOS.

For a system at a given volume V and temperature T, the Helmholtz free energy can be written as trinomial form,

$$F(V,T) = F_{\mathrm{c}}(V) + F_{\mathrm{n}}(V,T) + F_{\mathrm{e}}(V,T),$$

where $F_{\mathrm{c}}(V)$ represents the 0 K energy, $F_{\mathrm{n}}(V, T)$ is the vibrational free energy of lattice ions, and $F_{\mathrm{e}}(V, T)$ is the free energy due to thermal excitation of electrons. Other thermodynamic quantities can be obtained through the corresponding relations with $F(V, T)$. For example, the pressure is obtained via $P = -(\partial F/\partial V)_T$, entropy is obtained via $S = -(\partial F/\partial T)_V$, and internal energy is obtained via $E = F + TS$.

The supporting equations for the free energy are verbose and well described in Refs. [1,20−23]. An outline of the modifications made in the WEOS model, compared with those traditional forms, is as below:

- The Born-Mayer (BM) potential combined with six order polynomial is used to express the cold curve. The BM potential is well suited for describing the cold curve in low compression range. However, beyond this range, six-order polynomial, obtained by fitting cold free energy evaluated from BM at low compression ratio and TF [5−7] models including TF, TFD (Thomas-Fermi-Dirac model only with exchange corrections) and TFC (Thomas-Fermi Kalitkin model with quantum and exchange corrections) at high compressions ratio, is more suitable and flexible. The pressure and its first volume derivative are continuous at the transition density. We give three sets of parameters, WEOS_TF, WEOS_TFD and WEOS_TFC, for one material, these parameters are kept the same below the transition density;
- The ionic term is expressed by the modified Debye model [20] where the high-temperature anharmonic effects are taken into accounted via an empirical interpolation [22] between a perfect solid under normal conditions and an ideal gas. After these modifications, the WEOS becomes suitable for correctly describing the solid, liquid and gas states;
- The electronic term is described by Formula [20,21,23] at low temperature (usually lower than 10 ev or even more lower), and EOS of electrons are calculated by Rational Function Method of Interpolation [24] from the theoretical database of TF models at high temperature.

There are about thirteen unknown parameters in the WEOS model and they are fitted using both theoretical and experimental data. The strategy of calibration of the WEOS model includes fitting experimental data on shock compression of solid density by least squares, optimizing two potential parameters of BM by the golden cross method until the least square deviation of the theoretical from experimental Hugoniot, determining the anharmonic factor and Grüneisen coefficient by comparing the Hugoniot of dense and porous density, obtaining six coefficients of polynomial by fitting cold curve from BM and TF models, interpolating electronic EOS from TF and TFC theoretical data, solving the volume of fusion and volume of gasification by the melting and boiling temperature at $P = 1$ atm. Finally, one must check the pressure, bulk modulus and Grüneisen coefficient at ambient condition.

In consideration of the accuracy of data and the range of pressure, we choose about 170 Hugoniot data from Refs. [25−28] and then fit them by polynomial regression. The shock velocity-particle velocity (D-u_P) relation of copper which is used in the calibration the WEOS model up to 990 GPa is $D = 3.899 + 1.52\ u_P - 0.009\ u_p{}^2$.

Until now we have studied nearly 40 elements which are marked by red color in period table in Fig. 1.

3. The validation formalism for the WEOS

Two key points here are the accuracy of the WEOS and the way to validate it. Due to the complicated physics and limitation of modern theoretical models of the thermodynamics of extreme states, only relatively limited phase states are accessible according to rigorous theoretical model. Therefore, the range of validity of the WEOS is restricted by the nature of the physical approximations. We focus our attention to the comparison with the available calculations by rigorous theoretical models and experimental data which have not been used in the procedure of calibration.

The thermodynamic consistency is always kept because all thermodynamic properties are derived from the free energy. The procedure of validation includes comparisons between the WEOS calculations and each one of the followings: the results of ab initio cold curve, the room-temperature isotherms from experiment, other semi-empirical models and electronic structure theories, experimental data on shock compression of dense and porous copper, off-Hugoniot information corresponding to the double shock in reflected shock wave and to adiabatic expansion of shock-compressed copper, measurements of the sound velocity in shock-compressed copper.

3.1. The ab initio cold curve

The density functional theory (DFT) [29,30] calculations are widely used in the high-pressure research. At room

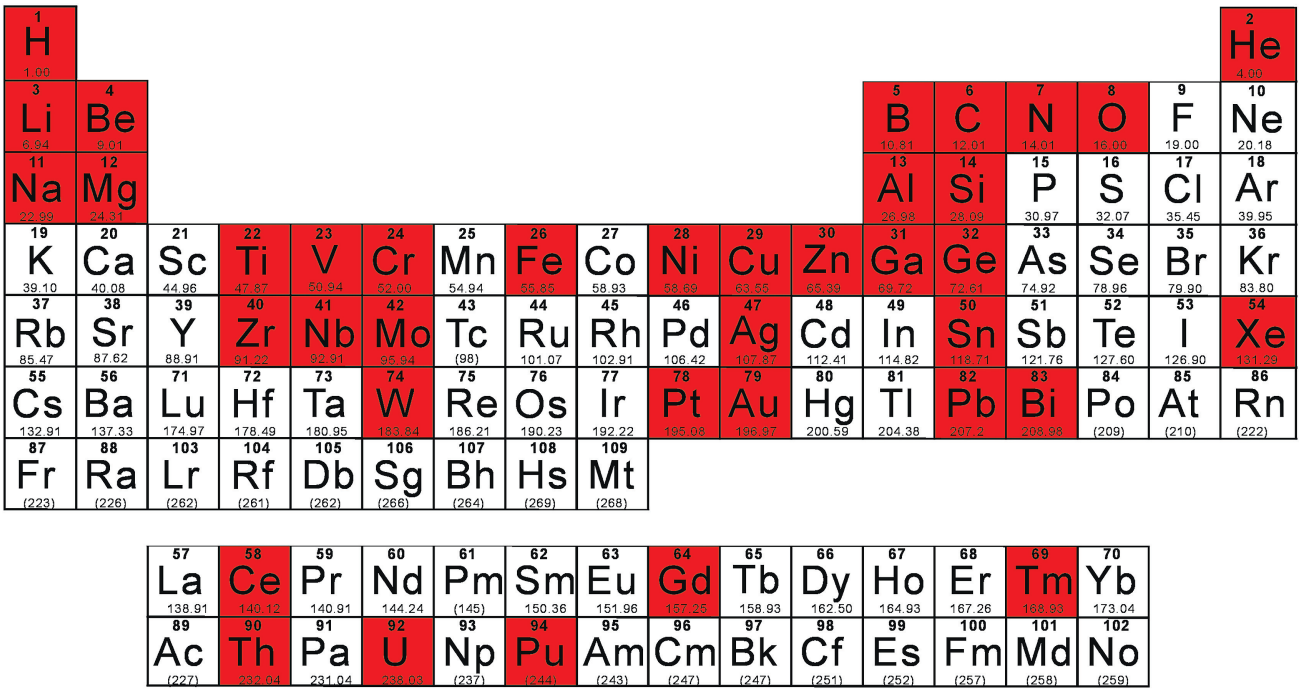

Fig. 1. The WEOS of elements marked by red color in periodic table have been evaluated.

pressure and temperature, the lattice structure of copper is FCC (face-centered cubic). The static compression to 190 GPa [31] and theoretical investigation [32] to 100 TPa show no structure phase transition. In order to estimate effect of electronic partitioning between core and band states, we calculated the cold energy and pressure of copper with the use of two ab initio methods, the first is the plane wave pseudo-potential VASP [33] and the second is the full potential WIEN2K [34,35]. We use the generalized gradient approximation (GGA) [36,37] for the exchange-correlation functional in both calculations. We test kinetic-energy cutoff and k-point sampling to assure a total energy convergence of 1-meV per atom. As a result of the convergence tests, the kinetic-energy cutoff is 360 eV and k-point meshes of Brillouin-zone sampling based on the Monkhorst-Pack scheme are 15^3 for VASP. The muffin-tin radii, the plane wave cutoff K_{cut} and the number of k-points use the same setting as in Ref. [38] for WIEN2K. The result is shown in Fig. 2. The equilibrium volume is 11.96 Å^3 and 12.13 Å^3 by VASP and WIEN2K, respectively. The experimental equilibrium volume is 11.81 Å^3 at the room-temperature. The relative volume differences between DFT and experiment are 1.3% and 2.7%, respectively. The pressures of pseudo-potential and full-potential calculations are up to 20700 GPa and 1600 GPa, respectively. The calculated cold curves and relative difference are shown in Fig. 2. It is seen that the relative difference is biggest near equilibrium volume, and then decreases with decreasing volume or increasing pressure. It is less than 3% up to pressure of 1600 GPa. Because of the dominance of static energy, practical calculations based on DFT typically have errors of several percent in density at zero pressure [30]. These are unacceptably large errors for the purpose of high accuracy EOS. We didn't try to fix the error between ambient volume of experiment and DFT. In the WEOS, experimental ambient volume has been used to calibrate parameters. The result of ab initio can be a good test under compression.

The cold curves of the WEOS and VASP are shown in Fig. 3. In order to make quantitative comparisons, the relative differences are presented in Fig. 4, where $X = (V/V_0)^{1/3}$. Experimental and ab initio equilibrium volume V_0 are used in the WEOS model and VASP, respectively. As seen from Figs. 3 and 4, the relative difference between WEOS_TF and VASP is up to 30%, while for WEOS_TFD and WEOS_TFC it is less than 13% and 8% in the region of compression ratio from 2 to 6 or $0.55 < X < 0.793$. This contrast shows us that the cold curve of WEOS_TFC agrees ab initio cold curve better than WEOS_TF and WEOS_TFD under high pressure.

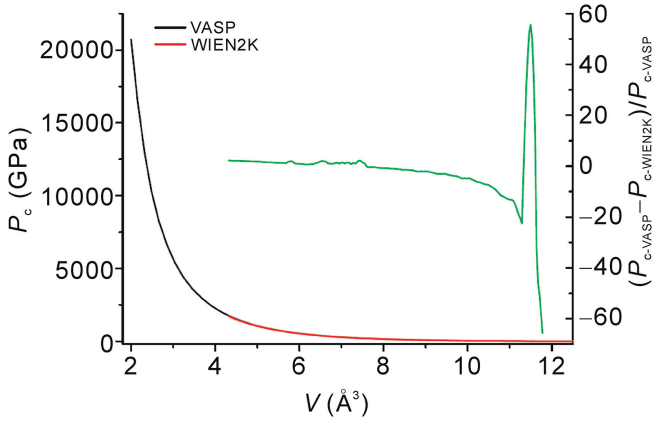

Fig. 2. The cold curve of copper calculated by VASP and WIEN2K. Green Line represents the relative difference.

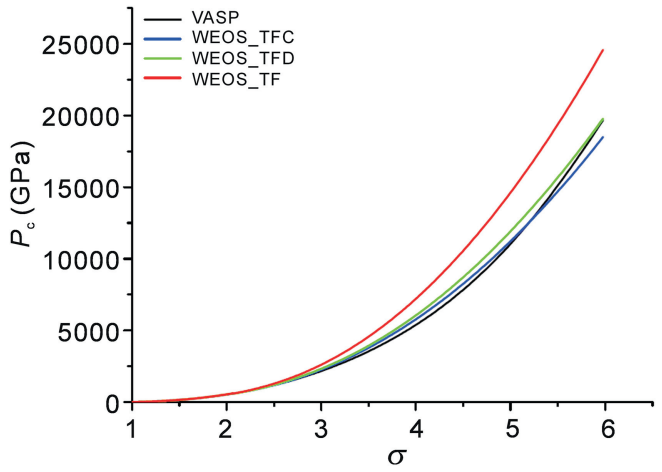

Fig. 3. Ab initio cold pressure versus compression ratio for Cu ($\sigma = V_0/V$-compression ratio).

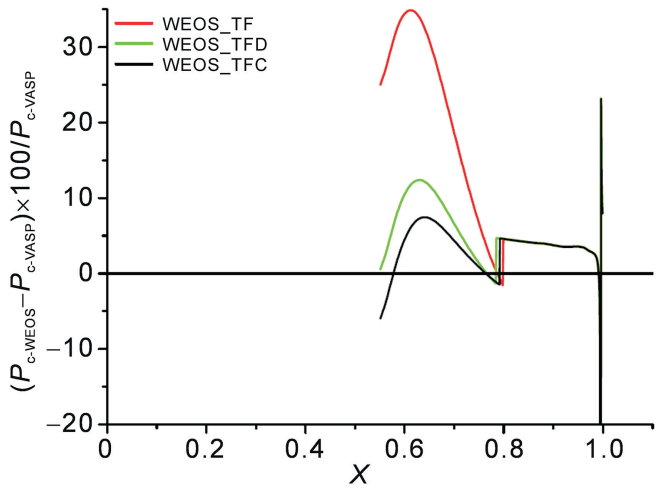

Fig. 4. The relative difference of cold pressure between the WEOS and VASP for Cu.

3.2. The room-temperature isotherm from semi-empirical methods

Reduced room-temperature isotherm of copper is given in works [39–48]. Their parameters were obtained using static [43–45] or reduced shock-wave [46–48] data, so the accuracy is insufficient outside the range of experimental data. EOS parameters [40–42] are very different, even though those authors resorted to the most reliable theoretical and experimental data that they found. Kalitkin [39] used more restrictions to determine the room-temperature isotherm parameters and gave two sets of parameter corresponding different forms. In fact, the pressures of these two isotherms have a little difference which is not larger than 2%. The curve Kalitkin20042 [39] is recommended as the standard because it is obtained using four conditions to define the parameter of cold pressure. The four conditions are as follows: at the normal state, the pressure is zero; the isotherm and the Hugoniot curves have the same initial slope; the TF model is valid at high compression; the relative difference between the quantum-statistical (QS) and TF models is reasonable. The relative deviations between the room-temperature isotherm recommended by Kalitkin [39] and other models are shown in Fig. 5. It demonstrates that all errors are less than 15%, most errors less than 5% at low ($\sigma < 2$ or $X > 0.793$) and at high pressure ($\sigma > 20$ or $X < 0.368$). Meanwhile, the largest errors are up to 30% in the range of $2<\sigma < 20$ or $0.368 < X < 0.793$. This means that experiments at low pressure and theoretical data at high pressure can be reproduced by semi-empirical models, but the isotherm in the intermediate range depends on the interpolating and fitting methods.

In order to further quantitatively validate the WEOS, the room-temperature isotherms by TF models and mean-field potential approach (MFP) [38,49] are calculated. We choose the same standard as Kalitkin20042, the relative errors of the WEOS, TF models, MFP are shown in Fig. 6. Fig. 6 shows that the relative errors of three TF models decrease with increasing pressure and approach the correct limits at infinity pressure; the relative error of the WEOS are less than 5% at low pressure ($\sigma < 2$); the relative errors of the WEOS and theoretical data of TF models are less than 5% in range of compression ratio $6 <\sigma < 20$ ($0.368 < X < 0.550$). This is not surprising for the last one, because the theoretical data are used in this range to calibrate parameters of the WEOS. Greeff, et al. [32] investigated room temperature isotherm of FCC Cu at high pressure by the linear combinations of Gaussian-type orbitals-fitting function (GTOFF) method [50] with thermal correction. This electronic structure theory is unlike the above DFT. It requires neither spatial partitioning, between muffin-tin and interstitial regions, nor electronic partitioning, between core and band states. Also, the relative differences between Ref. [32] and Kalitkin20042 in Ref. [39] are shown in Fig. 6. The largest difference is 6.9% at $\sigma = 5.9$

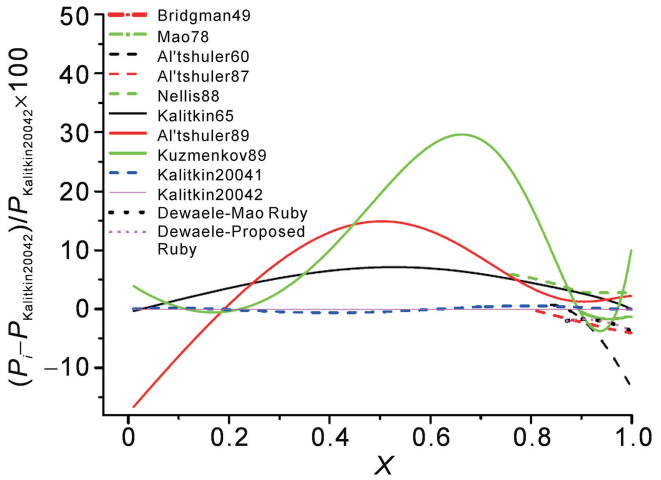

Fig. 5. Deviations from Kalitkin's standard isotherm [39]. The pink straight line corresponds to zero (the standard recommended, Kalitkin20042), the blue dash line is another isotherm by Kalitkin, the black, red and green solid lines represent previous approximations of different authors [40–42], two dot lines represent static experiment recommended by Dewaele in 2004 [45], other dashes represent previous static or related experiment [43,44,46–48].

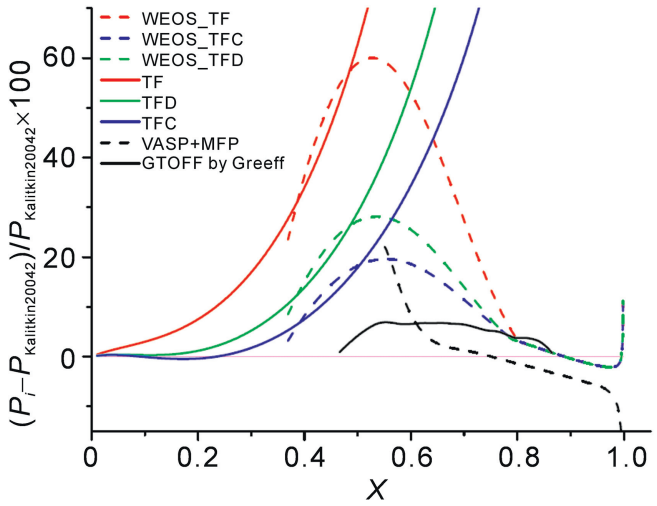

Fig. 6. Deviations from Kalitkin's standard isotherm. The pink straight line is zero as described in Fig. 5, The red, green and blue dash lines represent three cases of the WEOS. The black dash line represents result of MFP with VASP. The black solid line represent calculation of GTOFF code by Greeff [32]. The red, green and blue solid lines represent results of TF models.

or $X = 0.553$. The relative error of MFP increases with increasing pressure, and a sudden increase occurs at $\sigma = 4.8$ ($X = 0.592$). It indicates that the effect of electronic partitioning between core and band states may be arising in our ab initio calculation of pseudo-potential under extreme high compression.

The WEOS agrees with the standard isotherm recommended by Kalitkin at lower pressure and reproduce theoretical data of TF models at higher pressure. However, the deviations between WEOS and the standard isotherm are obvious at middle pressure. Meanwhile, it is worth to note that the room-temperature isotherm in range $2 < \sigma < 20$ is diffusive for the WEOS, ab initio and other electronic structure theory [32]. There is still no any precise experimental data to validate these models according to our knowledge. The isentropic compression experiment [51] makes it possible to obtain a reasonable data which can be used to valid the theoretical model in this regime.

3.3. Hugoniot curves for dense and porous initial states

We calculate the Hugoniot which is a locus of points achievable under shock conditions, generally from ambient conditions. We find the root (specific volume or inverse density) from the following equation:

$$e_H - e_0 + (P_0 + P_H)(V_H - V_0)/2 = 0$$

where e, P, V are specific energy, pressure and specific volume, respectively. V_0 and P_0 are the initial volume and pressure, V_H and P_H are the volume and pressure points along the Hugoniot. Since $P(\rho, T)$ and $e(\rho, T)$ are constrained by a given temperature, the density becomes the dependent variable. Therefore, one can give Hugoniot by solving routine the arrays of density, temperature, pressure $P(\rho, T)$, energy $e(\rho, T)$, and a temperature grid along which to search for Hugoniot points. The principal Hugoniot for copper is shown in Fig. 7 as function of pressure on compression ratio.

In Fig. 7, the experimental data correspond to five kinds of techniques which have been used to perform dynamic shock-wave compression experiments. The five kinds of techniques include chemical explosive drivers [25,52,53], light gas guns [26,28,54], explosively driven striker plates [27,46,66], nuclear explosions [54,55,58,63] and laser [71,72]. It is seen that the oldest data [56] have been obtained by Al'tshuler in 1958 and the newest data [71,72] by Fu in 2007. Fig. 7 shows that the newer data agrees with the older data, but are less scattered below 1000 GPa. Meanwhile, the newest laser-driven shock data are much more scattered than the older data. The WEOS has been calibrated by the precise experimental data up to 990 GPa. So it reproduces experimental data well. We didn't calibrate the WEOS by substantially high pressure above $\sigma = 2.1$. But the experimental data fall well in the WEOS_TF and WEOS_TFC. It means that the experimental uncertainties are too large to discriminate which one is better between TF and TFC theory.

Fig. 8 shows the Hugoniot curves for porous copper. The porosity degree is defined as $m = \rho_0 / \rho_{00}$, where ρ_0 is normal density of dense copper and ρ_{00} is the density of porous copper. It is seen that the WEOS agrees with most experimental data.

3.4. Off-Hugoniot states for copper

Off-Hugoniot states of matter can be obtained by double-shocking of a material or by allowing a shock-compressed material to release isentropically. It is important to obtain EOS data off the principal Hugoniot in order to obtain greater constraints on models for thermal pressure [73]. Nellis [73] used Ta as impactor and used Al and Ta as anvils to obtain data on double-shock compression and isentropic release. Glushak [27], Zhernokletov [68], and Bakanova [74] obtained data on isentropic expansion of shocked metal. With

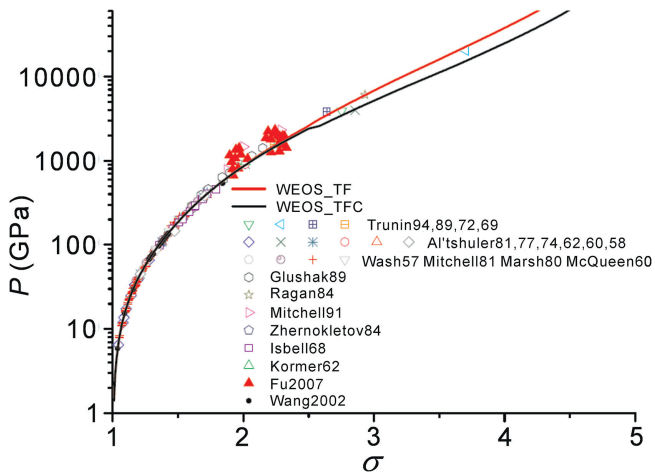

Fig. 7. The principal Hugoniot of copper. The black and red solid lines represent two cases of the WEOS. The scattered points represent experimental data from Refs. [25–28,52–72].

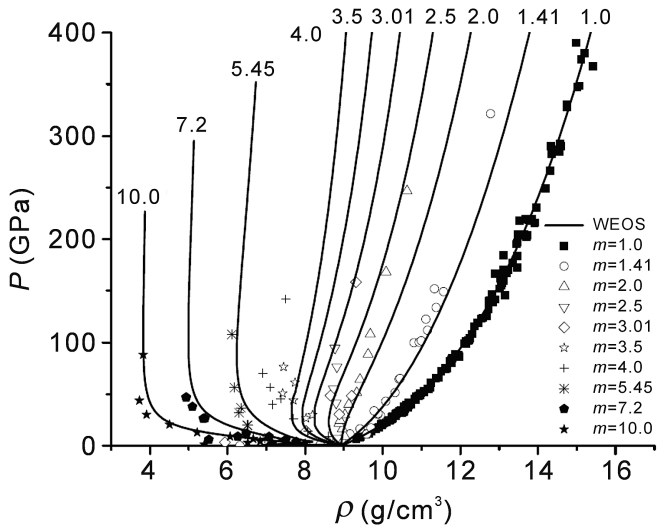

Fig. 8. Hugoniot pressure versus density for dense and porous copper. The solid lines represent calculations of the WEOS. The numbers near curves are the porosity degree. The scatter points represent experimental data from Refs. [23,25–27,69,70,75].

the initial density calculated from the particle velocity, the pressure and the initial density measured in experiment, we can evaluate the first-shock state, mirror reflection, reshock and release adiabatic path in the WEOS. All double-shock and release states of Cu from the WEOS together with experimental data are plotted in Fig. 9 as P versus u_P and compared with the mirror reflection of the principal Hugoniot about that first-shock state. Fig. 9 demonstrates that the mirror reflection and double-shock or release state are very close near the principal Hugoniot. These two points measured by Nellis agree with both curves within the experimental uncertainties of 4.0% in pressure and 2.9% in particle velocity (calculated by data of table 5, 3% and 2.5% were given in text in Ref. [73]). Three experiments [68,74] at the lower first-shock pressures are all in excellent agreement with the WEOS. The first-shock state for four points in the middle range of pressure has tiny deviation from the WEOS. We infer that because different Hugoniots are used in Refs. [27,68,74], but the WEOS results still fall well in the experimental with scattered release state. As described in Sec. 2, off-Hugoniot data were not used to constrain the WEOS. So these comparisons are a good test of the model and parameters of the WEOS.

3.5. Sound velocity of shocked copper

Steinberg [76] et al. investigated the constitutive model and gave the Steinberg-Guinan (SG) constitutive relation for many metals including copper. In Fig. 10, the bulk and longitudinal sound velocities C_b and C_l calculated by the WEOS and the shear modulus of SG [76] are shown in red and black solid curves, respectively, and compared with experimental data [75–85]. It is seen that the sound velocity experimental data [77] are more scattered than room-temperature static and Hugoniot data. The longitudinal sound velocity rises gradually with increasing pressure along the Hugoniot and then drops near the shock melting point. The theoretical bulk sound velocities from the WEOS agree well with most experiments, but the longitudinal sound velocities increase with increasing shock pressure and not ceases just as experimental data [77]. The longitudinal sound velocity ceases increasing near shock melting point. This suggests shear softening [86] which is observed on Mo by Nguyen et al. This deviation from the prediction of the SG and the WEOS model in the Hayes data above 100 GPa suggests that it is necessary to fix shear modulus in the SG model or develop a new theory that incorporates near-solidus shear softening.

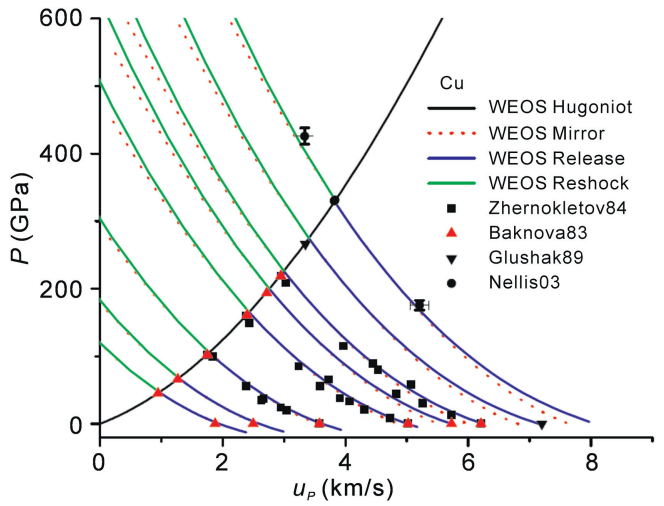

Fig. 9. Shock pressure – particle velocity plot for copper. Lines – are calculation results of the WEOS. Points – are experimental data from Refs. [27,68,73,74].

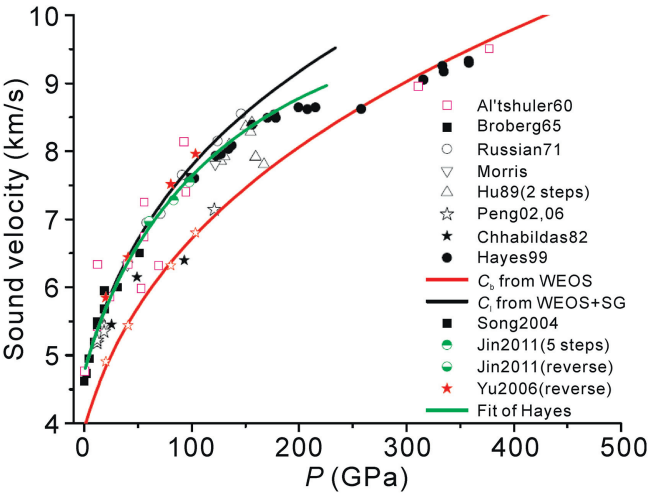

Fig. 10. The bulk and longitudinal sound velocities versus pressure curves of copper. The red and black solid lines represent the present calculation. The green line are fitting of Hayes data [77]. Points are experimental data from Refs. [77–86].

4. Summary

We proposed the formalism for validating the WEOS of copper in a wide regime. The results show that the developed WEOS, especially WEOS_TFC, reproduces the ab initio cold curve under compression, room-temperature static isotherm. Most Hugoniot data for dense and porous samples and sound velocity data agree the results of WEOS well. Hugoniot data at substantially high pressure above $\sigma = 2.1$ fall well in the result of WEOS_TF and WEOS_TFC. These give us confidence in the accuracy of the WEOS, which is important for validation and verification of EOS in high temperature and pressure technology.

The distinct divergence for the room-temperature isotherm between $2 < \sigma < 6$ exists for the WEOS, the standard isotherm, ab initio and other electronic structure theory. The isentropic compression experiment will give reasonable data which can be used to validate the theoretical model in this regime.

For substantially high pressure above $\sigma = 2.1$, the experimental data fall well in theoretical results between WEOS_TF and WEOS_TFC. But the experimental data are too diffusive to discriminate which theory (TF or TFC) is better. The use of laser-driven and magnetic driven shock waves make it possible to obtain states of matter with extremely high energy densities and pressure of TPa in laboratory. The information gained in these dynamic experiments will substantially broaden our basic notions about the physical properties of matter, particularly in the extreme high pressure.

There is a disagreement in the longitudinal sound velocity between the prediction and experimental data [77]. The correction of the SG constitutive model or development of new theory that incorporates near-solidus shear softening is needed.

Acknowledgments

We thank our collaborators Yuyin Yu, Ke Jin, Xiang Wang and Xiuguang Huang for permitting us to use their experimental data, and we thank our anonymous reviewers and editor for their thoughtful comment, which improved this paper.

This work was supported by the National Natural Science Foundation of China (Nos. 10804011, 11176002).

References

[1] V. Bushman, G.I. Kanel, A.L. Ni, V.E. Fortov, Intense Dynamic Loading of Condensed Matter, Taylor&Francis, London, 1993.

[2] M.D. Knudson, M.P. Desjarlais, Adiabatic release measurements in aluminum between 400 and 1200 GPa: characterization of aluminum as a shock standard in the multimegabar regime, Phys. Rev. B 91 (2015) 224105.

[3] H.K. Mao, R.J. Hemley, Ultrahigh pressure transitions in solid hydrogen, Rev. Mod. Phys. 66 (1994) 671.

[4] T. Kimura, N. Ozaki, T. Okuchi, T. Mashimo, K. Miyanishi, et al., Static compression experiments for advanced coupling techniques of laser-driven dynamic compression and precompression target, J. Phys. Conf. Ser. 215 (2010) 012152.

[5] R.P. Feymnan, N. Metropolis, E. Teller, Equations of state of elements based on the generalized Fermi-Thomas theory, Phys. Rev. 75 (10) (1949) 1561−1573.

[6] S.L. McCarthy, The Kirzhnits Corrections to the Thomas-Fermi Equation of State, Lawrence Livermore Laboratory, 1965. Report UCRL-14364.

[7] D.A. Kirzhnits, Y.E. Lozovik, G.V. Shpatakovskaya, Statistical model of matter, Soviet Physics Uspekhi 18 (1975) 649.

[8] A.F. Nikiforov, V.G. Novikov, V.B. Uvarov, Quantum-statistical Models of Hot Dense Matter: Methods for Computation Opacity and Equation of State, vol. 37, Springer Science & Business Media, 2006.

[9] W. Ebeling, A. Forster, V.E. Fortov, V.K. Gryaznov, A.Y. Polishchuk, Thermophysical Properties of Hot Dense Plasmas, B. G. Teubner, Verlagsgesellschaft, Stuttgart Leipzig, 1991.

[10] D.C. Wallace, Statistical Physics of Crystals and Liquids, World Scientific, Singapore, 2003.

[11] W. Lorenzen, B. Holst, R. Redmer, Demixing of hydrogen and helium at megabar pressures, Phys. Rev. Lett. 102 (2009) 115701.

[12] S.A. Bonev, B. Militzer, G. Galli, Ab initio simulations of dense liquid deuterium: comparison with gas-gun shock-wave experiments, Phys. Rev. B 69 (2004) 014101.

[13] L.A. Collins, S.R. Bickham, J.D. Kress, S. Mazevet, T.J. Lenosky, et al., Dynamical and optical properties of warm dense hydrogen, Phys. Rev. B 63 (2001) 184110.

[14] M.P. Desjarlais, Density-functional calculations of the liquid deuterium Hugoniot, reshock, and reverberation timing, Phys. Rev. B 68 (2003) 064204.

[15] K.T. Delaney, C. Pierleoni, D.M. Ceperley, Quantum Monte Carlo simulation of the high-pressure molecular-atomic crossover in fluid hydrogen, Phys. Rev. Lett. 97 (2006) 235702.

[16] B. Militzer, D.M. Ceperley, J.D. Kress, J.D. Johnson, L.A. Collins, et al., Calculation of a deuterium double shock Hugoniot from Ab initio simulations, Phys. Rev. Lett. 87 (2001) 275502.

[17] F. Lin, M.A. Morales, K.T. Delaney, C. Pierleoni, R.M. Martin, et al., Electrical conductivity of high-pressure liquid hydrogen by quantum Monte Carlo methods, Phys. Rev. Lett. 103 (2009) 256401.

[18] S.P. Lyon, J.D. Johnson, SESAME: The Los Alamos National Laboratory Equation of State Database, Los Alamos National Laboratory, Los Alamos, NM, 1992. Technical report LA-UR-92-3407.

[19] R.M. More, K.H. Warren, D.A. Young, G.B. Zimmerman, A new quotidian equation of state (QEOS) for hot dense matter, Phys. Fluids 31 (10) (Oct. 1988) 3059−3078.

[20] Xishen Xu, Wanxiang Zhang, Theoretical Introduction to Equation of State, Scientific Press, Beijing, 1986 (in Chinese).

[21] Haifeng Liu, Haifeng Song, Gongmu Zhang, The single phase and two-phase equations of state for aluminum, AIP Conf. Proc. 1426 (2012) 832−835.

[22] N.N. Kalitkin, L.V. Kuz'mina, Russ. J., Plasma Phys. 2 (5) (1976) 478. Transl. from Fiz. Plazmy 2(5), 858−868.

[23] S.B. Kormer, A.I. Funtikov, V.D. Urlin, A.N. Kolesnikova, Dynamical compression of porous metals and the equation of state with variable specific heat at high temperatures, Zh. Eksp. Teor. Fiz. 42 (1962) 686−701 (in Russian) (Sov. Phys. JETP 15, 477-488(1962)).

[24] G.I. Kerley, Rational Function Method of Interpolation, LA-6903-MS, 1977.

[25] S.P. Marsh (Ed.), LASL Shock Hugoniot Data, Univ. California Press, Berkeley, 1980.

[26] A.C. Mitchell, W.J. Nellis, Shock compression of aluminum, copper and tantalum, J. Appl. Phys. 52 (1981) 3363−3374.

[27] B.L. Glushak, A.P. Zharkov, M.V. Zhernokletov, V. Ya. Ternovoi, A.S. Filimonov, et al., Experimental investigation of the thermodynamics of dense plasmas formed from metals at high energy concentrations, Sov. Phys. JETP 69 (4) (1989) 739−749.

[28] Xiang Wang, Summary of Technique in measurement of Equation of State, Report in Institute of Fluid Physics, 2002 (unpublished).

[29] P. Hohenberg, W. Kohn, Inhomogeneous electron gas, Phys. Rev. 136 (1964) B864.

[30] A. Khein, D.J. Umrigar, All-electron study of gradient corrections to the local-density functional in metallic systems, Phys. Rev. B 51 (1995) 4105.

[31] P.M. Bell, Ji-an Xu, H.K. Mao, Static compression of gold and copper and calibration of the ruby pressure scale to pressures to 1.8 megabars

(static. RNO), Shock Waves Condens. Matter (1986) 125−130. Springer US.
[32] C.W. Greeff, J.C. Boettger, M.J. Graf, J.D. Johnson, Theoretical investigation of the Cu EOS standard, J. Phys. Chem. Sol. 67 (2006) 2033−2040.
[33] G. Kress, J. Hafner, Ab initio molecular dynamics for open-shell transition metals, Phys. Rev. B 48 (1993) 13115. G. Kress and J. Furthmuller, Efficient iterative schemes for ab initio total-energy calculations using a plane-wave basis set, Phys. Rev. B54, 11169(1996); Efficiency of ab-initio total energy calculations for metals and semiconductors using a plane-wave basis set, Comput. Mater. Sci. 6, 15(1996).
[34] P. Blaha, K. Schwarz, P. Sorantin, S.B. Trickey, Full-potential, linearized augmented plane wave programs for crystalline systems, Comput. Phys. Commun. 59 (399) (1990).
[35] K. Schwarz, P. Blaha, G. Madsen, Electronic Structure calculations of solids using Wien2k package for material sciences, Comput. Phys. Commun. 147 (2002) 71.
[36] J.P. Perdew, K. Burke, M. Ernzerhof, Generalized gradient approximation made simple, Phys. Rev. Lett. 77 (1996) 3865.
[37] J.P. Perdew, K. Burke, M. Ernzerhof, Generalized gradient approximation made simple [Phys. Rev. Lett. 77, 3865 (1996)], Phys. Rev. Lett. 78 (1997) 1396.
[38] Y. Wang, D. Chen, X. Zhang, Calculated equation of state of Al, Cu, Ta, Mo, and W to 1000 GPa, Phys. Rev. Lett. 84 (2000) 3220.
[39] N.N. Kalitkin, L.V. Kuzmina, in: V.E. Fortov, L.V. Al'tshuler, R.F. Trunin, A.I. Funtikov (Eds.), Wide-range Characteristic Thermodynamic Curves, in High Pressure Shock Compression of Solids VII, Springer, 2004.
[40] L.V. Al'tshuler, S.E. Brusnikin, High. Temp. 27 (1) (1989) 39−47.
[41] N.N. Kalitkin, I.A. Govorukhina, Sov. Phys. Solid State 7 (2) (1965) 287−292.
[42] E.A. Kuzmenkov, Izv. Sib. Div. Russ. Acad. Sci. 6 (1989) 106−112.
[43] P.W. Bridgman, Proc. Am. Acad. Sci. 76 (6) (1949) 189.
[44] H.K. Mao, P.M. Bell, J.W. Shaner, D.J. Steinberg, Specific volume measurements of Cu, Mo, Pd, and Ag and calibration of the ruby R 1fluorescence pressure gauge from 0.06 to 1 Mbar, J. Appl. Phys. 49 (6) (1978), 3276−3283.
[45] A. Dewaele, P. Loubeyre, M. Mezouar, Equations of state of six metals above 94GPa, Phys. Rev. B70 (2004) 094112.
[46] L.V. Al'tshuler, S.B. Kormer, A.A. Bakanova, R.F. Trunin, Equations of state for aluminum, copper and lead in the high pressure region, Sov. Phys. JETP 11 (1960) 573−579.
[47] W.J. Nellis, J.A. Moriarty, A.C. Mitchell, Metals physics at ultrahigh pressure: aluminum, copper, and lead as prototypes, Phys. Rev. Lett. 60 (1988) 1414.
[48] L.V. Al'tshuler, S.E. Brusnikin, E.A. Kuzmenkov, J. Appl. Mech. Tech. Phys. 28 (1) (1987) 129−141.
[49] Song Haifeng, Haifeng Liu, Modified mean-field potential approach to the thermodynamic properties of a low-symmetry crystal: beryllium as a prototype, Phys. Rev. B 75 (2007) 245126.
[50] J.C. Boettger, Int. J. Quantum Chem. Sym 27 (1993) 147−154.
[51] J.-P. Davis, J.L. Brown, M.D. Knudson, R.W. Lemke, Analysis of shockless dynamic compression data on solids to multi-megabar pressures: application to tantalum, J. Appl. Phys. 116 (2014) 204903.
[52] J.M. Walsh, M.H. Rice, R.G. Mcqueen, F.L. Yarger, Shock-wave compressions of twenty-seven metals equations of state of metals, Phys. Rev. 108 (1957) 196−216.
[53] R.G. McQueen, S.P. Marsh, Equation of state for nineteen metallic elements, J. Appl. Phys. 31 (1960) 1253−1269.
[54] W.J. Mitchell, J.A. Nellis, R.A. Moriarty, N.C. Heinle, R. E. Tipton Holmes, G.W. Repp, Equation of state of Al, Cu, Mo, and Pb at shock pressures up to 2.4 TPa (24 Mbar), J. Appl. Phys. 69 (1991) 2981−2986.
[55] E. Ragan, Shock-wave experiment at threefold compression, Phys. Rev. Ser. A 29 (1984) 1391−1402.
[56] L.V. Al'tshuler, K.K. Krupnikov, M.I. Brazhnik, Dynamical compressibility of metals under pressure from 400000 to 4 million atmospheres, Sov. Phys. JETP 7 (1958) 614−618.
[57] L.V. Al'tshuler, A.A. Bakanova, R.F. Trunin, Shock adiabats and zero isotherms of seven metals at high pressures, Sov. Phys. JETP 15 (1962) 65−74.
[58] L.V. Al'tshuler, B.S. Chekin, Metrology of high pulsed pressures, in: Proceed. of 1 All-Union Pulsed Pressures Simposium, vol. 1, VNIIFTRI, Moscow, 1974, pp. 5−22 (in Russian).
[59] L.V. Al'tshuler, N.N. Kalitkin, L.V. Kuz'mina, B.S. Chekin, Shock adiabats for ultrahigh pressures, Sov. Phys. JETP 45 (1) (1977) 167−171.
[60] L.V. Al'tshuler, A.A. Bakanova, I.P. Dudoladov, E.A. Dynin, R.F. Trunin, et al., Shock adiabats for metals. New data, statistical analysis and general regularities, J. Appl. Mech. Tech. Phys. 22 (1981) 145.
[61] R.F. Trunin, M.A. Podurets, B.N. Moiseev, G.V. Simakov, L.V. Popov, Relative compressibility of copper, cadmium and lead at high pressures, Sov. Phys. JETP 29 (4) (1969) 630−631.
[62] R.F. Trunin, M.A. Podurets, G.V. Simakov, L.V. Popov, B.N. Moiseev, Experimental verification of the Thomas-Fermi model for metals under high pressure, Sov. Phys. JETP 35 (3) (1972) 550−552.
[63] R.F. Trunin, L.A. Il'kaeva, M.A. Podurets, L.V. Popov, B.V. Pechenkin, et al., Measurement of shock compressibility of iron, copper, lead and titanium at pressures of 20 TPa, Teplofiz. Vys. Temp. 32 (5) (1994) 692−695 (in Russian).
[64] R.F. Trunin, Shock compressibility of condensed matters in strong shock waves caused by underground nuclear explosions, Usp. Fiz. Nauk. 164 (11) (1994) 1215−1237 (in Russian).
[65] W.H. Isbell, F.H. Shipman, A.H. Jones, Hugoniot Equation of State Measurements for Eleven Materials to Five Megabars, General Motors Corp., Mat. Sci. Lab, 1968. Report MSL-68−13.
[66] S.B. Kormer, A.I. Funtikov, V.D. Ulrin, A.N. Kolesnikova, Dynamical compression of porous metals and the equation of state with variable specific heat at high temperatures, Sov. Phys. JETP 15 (1962) 477−478.
[67] R.F. Trunin, A.B. Medvedev, A.I. Funtikov, M.A. Podurets, G.V. Simakov, et al., Shock compression of porous iron, copper, and tungsten and their equation of state in terapascal pressure range, Sov. Phys. JETP 68 (2) (1989) 356−361.
[68] M.V. Zhernokletov, V.N. Zubarev, Yu. N. Sutulov, Adiabats of porous samples and expansion isentropes of copper, Zh. Prikl. Mekh. Tekhn. Fiz. 1 (1984) 119−123 (in Russian).
[69] R.F. Trunin, G.V. Simakov, Yu. N. Sutulov, A.B. Medvedev, B.D. Rogozkin, et al., Compression of porous metals in shock waves, Sov. Phys. JETP 69 (3) (1989) 580−588.
[70] V.K. Gryaznov, V.E. Fortov, M.V. Zhernokletov, G.V. Simakov, R.F. Trunin, et al., Shock compression and thermodynamics of highly nonideal metallic plasma, Sov. Phys. JETP 87 (4) (1998) 678−690.
[71] Sizu Fu, Xiuguang Huang, Minxun Ma, Hua Shu, Jiang Wu, et al., Analysis of measurement error in the experiment of laser equation of state with impedance-match way and the Hugoniot data of Cu up to ~2.24 TPa with high precision, J. Appl. Phys. 101 (2007) 043517.
[72] Xiuguang Huang, Sizu Fu, The Experiment of Laser Equation of State, Report in Shanghai Institute of Laser Plasma (unpublished), 2014.
[73] W.J. Nellis, A.C. Mitchell, D.A. Young, Equation-of-state measurements for aluminum, copper, and tantalum in the pressure range 80-440 GPa (0.8-4.4 Mbar), J. Appl. Phys. 93 (1) (2003) 304−310.
[74] Bakanova, I.P. Dudoladov, M.V. Zhernokletov, V.N. Zubarev, G.V. Simakov, On evaporation of shock-compressed metals under expansion, J. Appl. Mech. Tech. Phys. 24 (1983) 204.
[75] Yu. L. Alekseev, B.P. Ratnikov, A.P. Rybakov, Shock adiabats of porous metals, Zh. Prikl. Mekh. Tekhn. Fiz. 2 (1971) 101−106 (in Russian).
[76] D.J. Steinberg, S.G. Cochran, M.W. Guinan, A constitutive model for metals applicable at high strain rate, J. Appl. Phys. 51 (3) (1980) 1498−1503.
[77] D. Hayes, R. Hixson, R. McQueen, High pressure elastic properties, solid-liquid phase boundary and liquid equation of state from release wave measurement in shock-loaded copper, in: M.D. Furnish, L.C. Chhabildas, R.S. Hixson (Eds.), Shock Compression of Condensed Matter-1999, 2000, pp. 483−488. Melville, New York.
[78] Yuyin Yu, Measurement of Sound Velocity of Copper in Inverse Impact, Report in Institute of Fluid Physics, 2006 (unpublished).
[79] Pengjian Xiang, Comparative Study of Johnson-cook Constitutive Model and Steinberg Constitutive Model (Ph. D thesis), Graduate of China Academy Engineer Physics, Mianyang, 2006.

[80] Ke Jin, Measurement of Sound Velocity of Copper under shock loading, Report in Institute of Fluid Physics, 2012 (unpublished).
[81] Ping Song, Lingcang Cai, Xianming Zhou, Hua Tan, Experimental investigation of the release isentropes of OFHC copper, Chin. J. High Press. Phys. 19 (2) (2005) 174.
[82] L.V. Al'tshuler, S.B. Kormer, M.I. Brazhnik, L.A. Vladimirov, M.P. Speranskaya, et al., The isentropic compressibility of aluminum, copper, lead at high pressures, Sov. Phys. JETP 11 (4) (1960) 766−775.
[83] K.B. Broberg, Shock Wave in Elastic and Plastic Media, 1965.
[84] C.E. Morris, J.N. Fritz, B. E. Holian, LA-Ur -81.
[85] Jinbiao Hu, Qian Jingfu, Juxin Cheng, Sound velocities at high pressures and shock-melting of copper, Chin. J. High Press. Phys. 3 (3) (1989) 187.
[86] J.H. Nguyen, M.C. Akin, R. Chau, D.E. Fratanduono, W.P. Ambrose, et al., Molybdenum sound velocity and shear modulus softening under shock compression, Phys. Rev. B 89 (2014) 174109.